

NASA Contractor Report 172179

ICASE

NASA-CR-172179
19830026387

A ROTATIONALLY BIASED UPWIND DIFFERENCE SCHEME
FOR THE EULER EQUATIONS

Stephen F. Davis

Contract No. NAS1-17070
July 1983

INSTITUTE FOR COMPUTER APPLICATIONS IN SCIENCE AND ENGINEERING
NASA Langley Research Center, Hampton, Virginia 23665

Operated by the Universities Space Research Association



NF02532

NASA

National Aeronautics and
Space Administration

Langley Research Center
Hampton, Virginia 23665

LIBRARY COPY

SEP 14 1983

LANGLEY RESEARCH CENTER
LIBRARY, NASA
HAMPTON, VIRGINIA

A ROTATIONALLY BIASED UPWIND DIFFERENCE SCHEME
FOR THE EULER EQUATIONS

Stephen F. Davis
Institute for Computer Applications in Science and Engineering

ABSTRACT

The upwind difference schemes of Godunov, Osher, Roe and van Leer are able to resolve one-dimensional steady shocks for the Euler equations within one or two mesh intervals. Unfortunately, this resolution is lost in two dimensions when the shock crosses the computing grid at an oblique angle. To correct this problem, we develop a numerical scheme which automatically locates the angle at which a shock might be expected to cross the computing grid and then constructs separate finite difference formulas for the flux components normal and tangential to this direction.

We present numerical results which illustrate the ability of this new method to resolve steady oblique shocks.

Research supported by the National Aeronautics and Space Administration under NASA Contract No. NAS1-17070 while the author was in residence at ICASE, NASA Langley Research Center, Hampton, VA 23665.

1. Introduction

Beginning with the work of Godunov [2], considerable effort has been expended seeking numerical methods which can solve the equations of gas dynamics accurately and sharply resolve discontinuities.

In the case of one-dimensional flows containing steady discontinuities, this effort has paid off. Work by van Leer [14,15,16], Roe [12], Osher [1,11], Harten [5] and others indicates that the mechanism of "shock capture" is well understood and that it is now possible to design second order accurate schemes which resolve steady discontinuities within one or two mesh intervals without wiggles. A recent paper by Harten and Hyman [3] indicates that these results can be extended to one dimensional flows with moving discontinuities.

In the case of two dimensional flows, some progress has been made but there is room for improvement. It is well known that the one-dimensional results cited above can be reproduced in two-dimensional calculations if the computing grid is chosen so that only one set of grid lines crosses a discontinuity in the flow. This would appear to be the optimum way to account for the two-dimensional aspects of the flow but in practice it is very difficult to choose an appropriate grid either a priori or adaptively during a calculation. We shall not examine this approach here.

An alternative approach is to use dimensional splitting with a high resolution one-dimensional scheme in each split step. This method ignores the two-dimensional orientation of discontinuities but appears to work surprisingly well (cf. Yee et al. [18], Woodward and Collela [17]). Since this method is also simple to program, it is quite attractive for practical application.

Despite these attractions, we attempt to do better. In particular, in this paper, we derive a two-dimensional scheme which can sharply resolve weak

shocks which are skew to the fixed computing grid. Splitting methods have difficulty dealing with this situation. An outline of the paper follows.

In Section 2, we briefly discuss the ideas behind the Godunov [2] method and show heuristically why it resolves steady shocks so well. This is followed by an introduction to Godunov-type methods with particular emphasis on the flux vector splitting method of van Leer [16] which we later use.

In Section 3, we derive the numerical scheme. First we review the rotated difference scheme which Jameson [6] applied to the transonic full potential equation. Then we explain how rotated differences, properly applied, can improve shock resolution for the Euler equations. Finally, we construct normal and tangential fluxes for the Euler equations and show that the resulting method is in conservation form and is consistent with the conservation laws.

In section 4, we consider the choice of angle for the rotated differences. We present a choice which seems to be appropriate for shock resolution with the Euler equations and then we briefly discuss more general discontinuities and more general conservation laws.

Section 5 contains numerical computations using this scheme and comparisons with other schemes.

Section 6 summarizes the present work, discusses the results of the present work and presents an outline for future work.

2. Godunov-type Methods and One Dimensional Problems

In this section we study the Godunov method for one-dimensional systems of conservation laws

$$u_t + f(u)_x = 0 \quad (2.1)$$

In particular we wish to determine which features of this scheme are responsible for its ability to resolve steady discontinuities. This discussion follows closely that of Harten, Lax and van Leer [4], so the reader is encouraged to consult their paper for additional details.

The construction of Godunov's scheme is as follows. At discrete time levels t_n , $n = 0, 1, \dots$, the numerical approximation $v(x, t_n)$ to the solution $u(x, t_n)$ of (2.1) is taken to be a piecewise constant function of x , ie.

$$v(x, t_n) = v_j^n \quad \text{for } x \in I_j = ((j-1/2)\Delta x, (j+1/2)\Delta x) \quad (2.2)$$

To calculate the numerical approximation at the next time level $t_{n+1} = t_n + \Delta t$ we first solve exactly the initial value problem

$$u_t + f(u)_x = 0,$$

$$u(x, t_n) = v(x, t_n), \quad (2.3)$$

for $-\infty < x < \infty$ and $t_n < t < t_n + \Delta t$; and denote its solution by $u_n(x, t)$. This means that at each discontinuity of $v(x, t_n)$ we must solve a local Riemann problem. The solution to the Riemann problem at say the interface between I_j and I_{j+1} is a similarity solution which depends only on the states v_j^n and v_{j+1}^n and the ratio $(x - (j+1/2)\Delta x)/(t - t_n)$. We denote this solution by $u\{(x - (j+1/2)\Delta x)/(t - t_n); v_j^n, v_{j+1}^n\}$. Since signals propagate with finite velocity,

$$u\{(x - (j+1/2)\Delta x)/(t - t_n); v_j^n, v_{j+1}^n\} = v_j^n$$

when

$$(x-(j+1/2)\Delta x)/(t-t_n) < a_L$$

and

$$u\{(x-(j+1/2)\Delta x)/(t-t_n); v_j^n, v_{j+1}^n\} = v_{j+1}^n$$

when

$$(x-(j-1/2)\Delta x)/(t-t_n) > a_R \quad (2.4)$$

where a_L and a_R are the smallest and largest signal velocity respectively.

If we keep $(|a_{\max}|\Delta t)/\Delta x < 1/2$ where $|a_{\max}|$ is the largest signal speed, there will be no interaction between neighboring Riemann problems and $u_n(x, t)$ can be written exactly as

$$u_n(x, t) = u\{(x-(j+1/2)\Delta x)/(t-t_n); v_j^n, v_{j+1}^n\}$$

for

$$j\Delta x < x < (j+1)\Delta x, \quad t_n < t < t_{n+1} \quad (2.5)$$

To obtain a piecewise constant approximation $v(x, t_{n+1})$ for the next time step, Godunov averages $u_n(x, t_{n+1})$, i.e. he sets

$$v_j^{n+1} = 1/\Delta x \int_{I_j} u_n(x, t_{n+1}) dx \quad (2.6)$$

In terms of the solution to the local Riemann problems, we can rewrite this as

$$v_j^{n+1} = 1/\Delta x \int_0^{\Delta x/2} u(x/\Delta t; v_{j-1}^n, v_j^n) dx + 1/\Delta x \int_{-\Delta x/2}^0 u(x/\Delta t; v_j^n, v_j^{n+1}) dx \quad (2.7)$$

Since u_n is an exact solution to the conservation laws (2.1), we can evaluate the integral defining v_j^{n+1} in (2.6) by integrating (2.1) over $I_j^x(t_n, t_{n+1})$ to get

$$\int_{I_j} u_n(x, t_{n+1}) dx - \int_{I_j} u(x, t_n) dx + \int_{t_n}^{t_{n+1}} f(u_n((j+1/2)\Delta x, t)) dt - \int_{t_n}^{t_{n+1}} f(u_n((j-1/2)\Delta x, t)) dt = 0 \quad (2.8)$$

or

$$v_j^{n+1} = v_j^n - \frac{\Delta t}{\Delta x} [f(\hat{v}_{j+1/2}) - f(\hat{v}_{j-1/2})] \quad (2.9)$$

where

$$\hat{v}_{j+1/2} = u(0; v_j^n, v_{j+1}^n) \quad (2.10)$$

This shows that the Godunov method is in conservation form with numerical flux given by

$$f(v, \omega) = f(u(0; v, \omega)) \quad (2.11)$$

Next we examine how this scheme resolves stationary shocks. For the sake of clarity we consider only a single conservation law. Qualitatively similar results can be derived for systems of conservation laws (see Lax [8]) but the details are far more complicated.

A shock is an exact discontinuous solution to the Riemann problem of the form

$$u_n(x, t) = \begin{cases} u_L, & x < st \\ u_R, & x > st \end{cases} \quad (2.12)$$

where s satisfies the Rankine-Hugoniot jump condition

$$s(u_R - u_L) = f(u_R) - f(u_L) \quad (2.13)$$

and the entropy condition

$$a_L > s > a_R \quad (2.14)$$

where

$$a_L = \frac{df}{du}(u_L), \quad a_R = \frac{df}{du}(u_R) \quad (2.15)$$

A steady shock is a shock with $s=0$.

If the initial conditions represent a steady shock located on the boundary of a cell, ie.

$$v_j^0 = u_0(x, t_0) = \begin{cases} u_L & \text{for } x \in I_j \text{ and } j < 0 \\ u_R & \text{for } x \in I_j \text{ and } j \geq 0 \end{cases} \quad (2.16)$$

then equation (2.6) will be satisfied exactly for all time levels and (2.16) is an exact solution to Godunov's method.

If the initial conditions represent a steady shock located within a cell, say I_0 , then equation (2.6) will yield

$$v_j^0 = \begin{cases} u_L & \text{for } j < 0 \\ u_m & \text{for } j = 0 \\ u_R & \text{for } j > 0 \end{cases} \quad (2.17)$$

where u_m , is some intermediate value between u_L and u_R .

At time t_1 the solution to the Riemann problem at the interface between I_{-1} and I_0 will consist of a shock moving at the speed

$$s_L = \frac{f(u_m) - f(u_L)}{u_m - u_L} \quad (2.18)$$

If the shock is weak

$$f(u_m) \approx f(u_R) + \frac{df}{du}(u_R)(u_m - u_R) \approx f(u_R) + a_R(u_m - u_R) \quad (2.19)$$

Substitute this into (2.18) and note that $f(u_L) = f(u_R)$, so

$$S_L \approx a_R \frac{(u_m - u_R)}{(u_m - u_L)} \quad (2.20)$$

Since u_m is between u_L and u_R , $(u_m - u_R)$ and $(u_m - u_L)$ will have opposite signs and their quotient will be negative. Equation (2.14) with $s=0$, shows that a_R is negative. Thus S_L is positive, the shock moves to the right and by (2.10)

$$\hat{v}_{-1/2} = u(0; u_L, u_m) = u_L \quad (2.21)$$

Similarly, we see that the solution to the Riemann problem at the interface between I_0 and I_1 consists of a shock moving at the speed

$$S_R = \frac{f(u_R) - f(u_m)}{u_R - u_m} \quad (2.22)$$

If this shock is weak

$$f(u_m) \approx f(u_L) + \frac{df(u_L)}{du} (u_m - u_L) \approx f(u_L) + a_L (u_m - u_L) \quad (2.23)$$

Substituting (2.23) into (2.22) and using $f(u_L) = f(u_R)$ we obtain

$$S_R = a_L \frac{(u_L - u_m)}{(u_R - u_m)} \quad (2.24)$$

Since a_L is positive, by equation (2.14) with $s=0$ and $(u_L - u_m)$ and $(u_R - u_m)$ have opposite signs, S_R is negative and the shock moves to the left. Thus by (2.10)

$$\hat{v}_{1/2} = u(0; u_m, u_R) = u_R \quad (2.25)$$

Substitution of (2.21) and (2.25) into (2.9) yields

$$v_0^1 = v_0^0 - \frac{\Delta t}{\Delta x} [f(u_R) - f(u_L)] = v_0^0 \quad (2.26)$$

Thus (2.17) is an exact solution to Godunov's method.

We note in passing that the choice of numerical fluxes

$$f(u_L, u_m) = f(u_L)$$

and

$$f(u_m, u_R) = f(u_R)$$

which does not depend on u_m , confines the effect of the averaging which created u_m to a single cell. This would not be true of a conventional finite difference method whose numerical fluxes would depend on all of its arguments. Subsequent time steps would propagate the effect of u_m through the entire domain and thus spread the shock over many cells.

The construction of solutions of Riemann problems for nonlinear systems is a complicated iterative procedure. In addition, equations (2.9) and (2.10) show that, although the entire Riemann solution is computed, only its value at the cell interface is actually used. For this reason much recent research has been devoted to the construction of numerical flux functions which retain the shock capturing ability of Godunov's scheme but which are simpler to construct. A particularly simple approach to the construction of numerical flux functions for the Euler equations is the flux vector splitting of van Leer [16], which we now describe.

Van Leer splits the flux $f(w)$ into a forward flux $f^+(w)$ and a backward flux $f^-(w)$ which satisfies

1. $f(w) = f^+(w) + f^-(w)$
2. df^+/dw has all eigenvalues > 0 ; df^-/dw has all eigenvalues < 0
3. $f^\pm(w)$ is continuous with $f^+(w) = f(w)$ for Mach numbers $M \geq 1$ and $f^-(w) = f(w)$ for Mach numbers $M \leq -1$.
4. The components of f^+ and f^- together must mimic the symmetry of f with respect to M (all other state quantities held constant), that is $f_k^+(M) = \pm f_k^-(-M)$ if $f_k(M) = \pm f_k(-M)$.
5. df^\pm/dw must be continuous.
6. df^\pm/dw must have one eigenvalue vanish for $|M| < 1$.
7. $f^\pm(M)$, like $f(M)$, must be a polynomial in M , and of the lowest possible degree.

If the one dimensional fluxes for the Euler equations with ideal gas law are considered to be functions of density ρ , sound speed c and Mach number M , the resulting splittings are

- 1) mass

$$\rho u = \rho c M = \rho c \left\{ \frac{1}{2} (M+1) \right\}^2 - \rho c \left\{ \frac{1}{2} (-M+1) \right\}^2 \quad (2.27)$$

- 2) momentum

$$\begin{aligned} \rho u^2 + p &= \rho c^2 (M^2 + 1/\gamma) = \rho c^2 \left\{ \frac{1}{2} (M+1) \right\}^2 \left(\frac{\gamma-1}{\gamma} M + 2/\gamma \right) \\ &+ \rho c^2 \left\{ \frac{1}{2} (-M+1) \right\}^2 \left(-\frac{\gamma-1}{\gamma} M + 2/\gamma \right) \end{aligned} \quad (2.28)$$

- 3) total energy

$$\begin{aligned} (e+p)u &= \rho c^3 M \left(\frac{1}{2} M^2 + 1/(\gamma-1) \right) \\ &= \frac{\gamma^2}{2(\gamma^2-1)} \frac{(f^+_{\text{momentum}})^2}{(f^+_{\text{mass}})} + \frac{\gamma^2}{2(\gamma^2-1)} \frac{(f^-_{\text{momentum}})^2}{(f^-_{\text{mass}})} \end{aligned} \quad (2.29)$$

The reader is referred to van Leer's paper for a detailed derivation of these expressions. In addition, van Leer shows that these expressions satisfy the seven conditions stated above and that these conditions are sufficient to assure that steady shocks are resolved within two cells. The numerical flux based on this splitting is

$$f(u,v) = f^+(u) + f^-(v) \quad (2.30)$$

In the next section we incorporate this numerical flux into a two-dimensional rotated difference scheme.

3. Derivation of a Rotated Difference Scheme

In a supersonic region, the method of Murman and Cole [10] solves the transonic potential equation by replacing derivatives in the streamwise direction with upwind difference approximations and replacing derivatives in the direction normal to the streamlines with central difference approximations. This is easy to do when the computing grid is approximately aligned with the streamwise and normal directions but is difficult otherwise.

Jameson [6] overcomes this problem in the following way. He writes the transonic potential equation in a coordinate system aligned with and normal to the the local streamwise direction. He then expresses the derivatives in the streamwise-normal coordinate system in terms of derivatives in the coordinate system of his computing grid, making note of which terms come from streamwise derivatives and which terms come from normal derivatives. Finally, those terms which come from streamwise derivatives are approximated by upwind difference formulas and those terms which come from normal derivatives are approximated by central difference formulas. This creates a very effective method.

In the following we derive a method for the Euler equations which is based on this rotated difference idea. In particular, we attempt to choose a local coordinate system which permits us to apply the one dimensional theory of Section 2. This means that our local coordinate directions must be normal and tangential to potential shock directions. In Section 4 we show how to determine these directions. Here we assume that the directions are known and derive difference formulas that are based on these directions. We note in passing that shocks are approximately normal to the streamlines in transonic flows. Thus our choice of local coordinate system is equivalent to Jameson's in this case.

Consider a local cartesian coordinate system chosen as above. Such a coordinate system has coordinates (x',y') . The coordinate system of the computing grid, assumed for simplicity to be cartesian, has coordinates (x,y) . Dependent variables measured in the local and global coordinate systems are primed and unprimed respectively. This geometry is shown in Figure 1.

Since the Euler equations are invariant under rotation, they can be written immediately in the local coordinate system as

$$\frac{\partial U'}{\partial t} + \frac{\partial F'(U')}{\partial x'} + \frac{\partial G'(U')}{\partial y'} = 0 \quad (3.1)$$

where

$$U' = [\rho, \rho u', \rho v', e]^T$$

$$F' = [\rho u', \rho u'^2 + p, \rho u' v', (e+p)u']^T$$

$$G' = [\rho v', \rho u' v', \rho v'^2 + p, (e+p)v']^T \quad (3.2)$$

$$e = p/(\gamma-1) + 1/2 \rho(u'^2 + v'^2) \quad (3.3)$$

and

$$u' = u \cos\theta + v \sin\theta$$

$$v' = -u \sin\theta + v \cos\theta \quad (3.4)$$

In the vicinity of a plane steady shock, each of the terms in (3.1) is zero independently. We attempt to construct a numerical scheme which has the same property.

If we express the second term of (3.1) in global coordinates we get

$$\frac{\partial F'}{\partial x'} = \cos\theta \frac{\partial F'}{\partial x} + \sin\theta \frac{\partial F'}{\partial y} \quad (3.5)$$

This can be approximated by a finite difference expression

$$\begin{aligned} & \frac{\cos\theta}{\Delta x} [F'(U'_{i+1,j}, U'_{i,j}) - F'(U'_{i,j}, U'_{i-1,j})] \\ & + \frac{\sin\theta}{\Delta y} [F'(U'_{i,j+1}, U'_{i,j}) - F'(U'_{i,j}, U'_{i,j-1})] \end{aligned} \quad (3.6)$$

The conditions that this expression be zero across a steady shock independent of Δx and Δy are

$$[F'(U'_{i+1,j}, U'_{i,j}) - F'(U'_{i,j}, U'_{i-1,j})] = 0$$

and

$$[F'(U'_{i,j+1}, U'_{i,j}) - F'(U'_{i,j}, U'_{i,j-1})] = 0 \quad (3.7)$$

These relations are satisfied by the Godunov-type methods discussed in Section 2. For this reason, the F' fluxes should be approximated by Godunov-type numerical fluxes. We use the van Leer flux vector splitting but any other Godunov-type flux would suffice.

The third term in equation (3.1) says that G' is constant along lines which are parallel to a shock. To approximate this condition on a discrete grid we must make an assumption about the behavior of G' between grid points. For lack of any better information we assume that G' varies linearly between grid points.

A representative case is shown in Figure 2. We note that

$$-\tan\theta = \Delta x/\ell \quad (3.8)$$

so

$$\ell/\Delta y = \Delta x/(-\Delta y \tan\theta) = \frac{\Delta x \cos\theta}{\Delta y \sin\theta} \quad (3.9)$$

The condition that G' varies linearly between grid points can be written as

$$(G'_{i+1,j+1} - G'_{i+1,j})/\Delta y = (\tilde{G}' - G'_{i+1,j})/\ell$$

or

$$-(G'_{i+1,j} - \tilde{G}')\frac{\sin\theta}{\Delta x} + (G'_{i+1,j+1} - G'_{i+1,j})\frac{\cos\theta}{\Delta y} = 0 \quad (3.10)$$

The condition that G' be constant along a line parallel to a shock can be written

$$\tilde{G}' = G'_{i,j} \quad (3.11)$$

If we express the third term of equation (3.1) in global coordinates, we get

$$\frac{\partial G'}{\partial y'} = -\sin\theta \frac{\partial G'}{\partial x} + \cos\theta \frac{\partial G'}{\partial y} \quad (3.12)$$

We allow the numerical fluxes to depend on additional values of U' and approximate this expression by

$$\begin{aligned} & - \frac{\sin\theta}{\Delta x} [G'(U'_{i+1,j}, U'_{i+1,j\pm 1}, U'_{i,j}, U'_{i,j\pm 1}) \\ & - G'(U'_{i,j}, U'_{i,j\pm 1}, U'_{i-1,j}, U'_{i-1,j\pm 1})] \\ & + \frac{\cos\theta}{\Delta y} [G'(U'_{i,j}, U'_{i\pm 1,j}, U'_{i,j+1}, U'_{i\pm 1,j+1}) \\ & - G'(U'_{i,j-1}, U'_{i\pm 1,j-1}, U'_{i,j}, U'_{i\pm 1,j})] \end{aligned} \quad (3.13)$$

We then identify the numerical fluxes with the corresponding flux values in expression (3.10) and (3.11). If our linear interpolation assumption is correct, the resulting expression (3.13) is equal to zero.

We can derive many expressions that are similar to (3.10) and (3.11) and linear combinations of these can be used to construct numerical flux functions for (3.13). Thus the formulas presented below are not unique and much work is needed to determine which formulas are best.

To make our G' numerical flux look similar to our F' numerical flux, we split it up as follows:

$$\begin{aligned} G'(U'_{i+1,j}, U'_{i+1,j\pm 1}, U'_{i,j}, U'_{i,j\pm 1}) &= 1/2 [(1+Q)G'^+(U'_{i,j}, U'_{i,j\pm 1}) \\ & + (1-Q)G'^-(U'_{i+1,j}, U'_{i+1,j\pm 1})] \end{aligned} \quad (3.14)$$

Q is a parameter chosen to assure that the overall method remain stable. Current research is devoted to finding an optimal choice for this parameter and much remains to be done. Further discussion on the choice of Q appears in Section 5. Table 1 specifies how G^+ and G^- depend on the angle θ .

Until now we have discussed the derivation of numerical fluxes of local variables in local coordinate directions. To compute a global solution we need numerical fluxes of global variables in global coordinate directions. To obtain these we first express the flux of global variables in global coordinates in terms of the flux of local variables in local coordinates as shown below.

Case 1. Flux of a scalar variable

$$F_1(U) = \rho u = \rho u' \cos\theta - \rho v' \sin\theta = F'(U') \cos\theta - G'(U') \sin\theta$$

Case 2. Flux of a vector component

$$\begin{aligned} F_2(U) &= \rho u^2 + p = \rho(u' \cos\theta - v' \sin\theta)(u' \cos\theta - v' \sin\theta) + p \\ &= \rho u'^2 \cos^2\theta - 2\rho u'v' \cos\theta \sin\theta + \rho v'^2 \sin^2\theta + p(\cos^2\theta + \sin^2\theta) \\ &= F_2'(U') \cos^2\theta - G_2'(U') \cos\theta \sin\theta - G_3'(U') \cos\theta \sin\theta \\ &\quad + F_3'(U') \sin^2\theta \end{aligned} \tag{3.16}$$

The numerical flux is computed by replacing the local flux by its corresponding local numerical flux. The two cases shown demonstrate that the flux of a scalar variable, such as ρ or e , transforms like a vector or

first order cartesian tensor and the flux of a vector component, such as a momentum component, transforms like a second order cartesian tensor. These transformation laws are well known (cf. Segal [13]) and are easily programmed.

To summarize, if we are given an angle θ , we compute a numerical flux as follows:

- (1) Compute velocity components in the local coordinate system.
- (2) Compute normal and tangential numerical flux components in the local coordinate system as described above.
- (3) Use the cartesian tensor transformation laws to compute numerical flux components of the global variables in the global coordinate system.

We conclude this section with a brief discussion on what it means for a scheme to be conservative and consistent and thus show that the scheme described here possesses these characteristics.

A numerical scheme is called conservative if its numerical flux satisfies a discrete version of the divergence theorem. For a rectangular domain, this means that we must satisfy an identity of the form

$$\sum_{i=1}^N \sum_{j=1}^N \left[\frac{F_{i+1/2, j} - F_{i-1/2, j}}{\Delta x} + \frac{G_{i, j+1/2} - G_{i, j-1/2}}{\Delta y} \right] \Delta x \Delta y = \sum_{i=1}^N [F_{N+1/2, j} - F_{1/2, j}] \Delta y + \sum_{i=1}^N [G_{i, N+1/2} - G_{i, 1/2}] \Delta x \quad (3.17)$$

To satisfy this relation, we associate with each cell boundary point of the form $(x_{i+1/2}, y_j)$ a single numerical flux value $F_{i+1/2, j}$ and with each cell boundary point of the form $(x_i, y_{j+1/2})$ a single numerical flux value $G_{i, j+1/2}$. This assures that the expression on the left of (3.17) telescopes to give the expression on the right.

Since each numerical flux value depends on an angle θ , we associate a value of θ with each cell boundary point. The derivation of the tangential local flux G' assumed that θ was constant through a cell. This would indicate that we might prefer to associate the angle θ with cell centers rather than cell boundaries. Unfortunately we could not find a way to do this and maintain conservation.

Lax and Wendroff [7] have shown that a numerical scheme for hyperbolic conservation laws is consistent with the differential equations if the numerical flux reduces to the differential equation flux when all arguments of the numerical flux are set equal. That is

$$F(u,u,\dots,u) = F(u) \quad (3.18)$$

The scheme described here is derived so that (3.18) is satisfied by the numerical flux of local variables in local coordinates. Thus (3.18) is satisfied by the global numerical flux because both the global differential equation flux and the global numerical flux are computed from their respective local flux values by the same formulas.

4. Choice of Direction

In Section 3 we describe a method designed to resolve shocks by using different numerical flux functions in directions normal and tangential to shocks. In this section we show how to find these directions.

It is important to note that the algorithm we describe does not determine whether or not a shock exists. Thus it is not a shock-fitting algorithm. Instead the algorithm always assumes that a steady shock exists and computes

its normal direction. Our numerical tests indicate that this approach locates the proper direction when it is needed and causes no problems otherwise.

To determine the direction of a steady oblique shock, we note, as do Gasdynamics texts (cf. Liepmann and Roshko [9]), that a steady oblique shock can be studied as a normal shock with a superimposed uniform tangential velocity. Thus, if we are given two velocity vectors, we can locate a possible shock direction by finding a rotated coordinate frame in which both vectors have a common component.

A simple way to accomplish this was suggested by John Strikwerda. He pointed out that since the velocity in the tangential direction does not change across the shock, the shock must be normal to the velocity jump. That is, given two velocity vectors

$$\bar{v}(i-1, j) = [u(i-1, j), v(i-1, j)]$$

and

$$\bar{v}(i, j) = [u(i, j), v(i, j)]$$

the shock, if it exists, is normal to the direction of the vector

$$\delta_x \bar{v}(i, j) = [u(i, j) - u(i-1, j), v(i, j) - v(i-1, j)] = [\delta_x u, \delta_x v] \quad (4.1)$$

Thus the angle θ used to compute rotated numerical fluxes is

$$\theta = \arctan(\delta_x v / \delta_x u) \quad (4.2)$$

In practice, the velocity components are computed using a first order finite difference formula. In the smooth parts of the flow the error in the

velocity differences can be of the same order as the velocity differences themselves. This can cause the angle θ to vary wildly in a part of the flow field where little is happening. Numerical experiments indicate that this degrades the performance of the method.

To prevent this, we replace the velocity differences in equation (4.2) by weighted averages of the velocity differences at a number of points. At present we use the averaging

$$\delta_x u(i, j) = [\Delta_x u(i-1, j) + 4 \Delta_x u(i, j) + \Delta_x u(i+1, j)] / 6 \quad (4.3)$$

where

$$\begin{aligned} \Delta_x u(i, j) = \{ [u(i, j-1) - u(i-1, j-1)] + 4 [u(i, j) - u(i-1, j)] \\ + [u(i, j+1) - u(i-1, j+1)] \} / 6 \end{aligned} \quad (4.4)$$

and

$$\delta_y u(i, j) = [\Delta_y u(i, j-1) + 4 (\Delta_y u(i, j) + \Delta_y u(i, j+1))] / 6 \quad (4.5)$$

where

$$\begin{aligned} \Delta_y u(i, j) = \{ [u(i-1, j) - u(i-1, j-1)] + 4 [u(i, j) - u(i, j-1)] \\ + [u(i+1, j) - u(i+1, j-1)] \} / 6 \end{aligned} \quad (4.6)$$

Numerical tests indicate that this procedure locates the proper shock angles and provides smooth angle variations.

The disadvantage of this approach is that it locates steady shocks for the Euler equations but does not locate steady contact discontinuities for the Euler equations or steady discontinuities for other systems of conservation laws. This limitation is also true of the van Leer formulas that we used to compute numerical flux components in the normal direction. In the future we

plan to construct a method which can locate these more general discontinuities and to use the method of Roe [12] to resolve them.

One way that we might do this is to note that for the scalar equation

$$u_t + f(u)_x + g(u)_y = 0 \quad (4.7)$$

the normal flux is continuous across a steady discontinuity but the tangential flux is not. Therefore the discontinuity, if it exists, is located in the direction of the vector

$$\delta_{\vec{x}} \vec{F} = [f(i,j)-f(i-1,j), g(i,j)-g(i-1,j)] = [\delta_x f, \delta_x g]. \quad (4.8)$$

For systems we might take linear combinations of vectors like (4.8). One possibility for a system of m equations would be to seek potential discontinuities in the direction of the vector

$$\delta \vec{F} = \left[\sum_{j=1}^m \frac{(\delta f_j)(\delta u_j)}{(\delta u_j)^2}, \sum_{j=1}^m \frac{(\delta g_j)(\delta u_j)}{(\delta u_j)^2} \right] \quad (4.9)$$

Thus far no numerical experiments have been performed using equation (4.9).

Baines⁽¹⁾ has proposed another promising approach to the problem of locating general discontinuities. He chooses the angle which satisfies a discrete approximation to the equation

(1) M. T. Baines, 1982, University of Reading, Reading, England, personal communication.

$$\frac{\partial G'}{\partial y'} = -\sin\theta \frac{\partial G'}{\partial x} + \cos\theta \frac{\partial G'}{\partial y} = 0 \quad (4.10)$$

At this time, some details of this procedure need to be worked out and no numerical results are available.

5. Numerical Results

In this section we present some numerical computations which demonstrate the ability of the present first order method to resolve steady, oblique shocks. These results are compared with the results of computations using state-of-the-art first and second order upwind methods.

Consider the problem of supersonic flow over a wedge which is illustrated in Figure 3. The solution to this problem is a single oblique shock wave. We consider only cases where the flow is supersonic everywhere.

To solve this problem we construct a uniform computing grid aligned with the wedge as shown in Figure 4. We specify all variables at the left and top boundaries and we extrapolate all variables at the right boundary. These boundary conditions are correct at the left and right boundaries but the top boundary is overspecified since the normal velocity at this boundary is subsonic. Fortunately, for the cases considered here, no signals reach this boundary from inside the computational domain and this overspecification causes no difficulties.

At the lower boundary we specify that the velocity normal to the wall be zero and use some numerical procedure to specify the remaining variables at the wall. We have experimented with a number of numerical boundary condition procedures and have found that the following gives the best results, at least for the methods and problems considered here.

To compute the pressure and density at the wall, we follow Chakravarty and Osher [1] and assume that locally, only simple plane waves leave the boundary. In this case the relations

$$c - \frac{(\gamma-1)}{2}v = \text{const.}$$

$$p/\rho^\gamma = \text{const.}$$

$$c = \sqrt{\frac{\gamma p}{\rho}} \quad (5.1)$$

which are satisfied along the characteristics that reach the wall from the interior, and the wall boundary condition, $v=0$, determine the pressure and density at the wall.

Various schemes have been used to determine the tangential velocity at the wall. Here we use the condition that, in the steady state the total enthalpy along the wall should be constant. This gives a relation

$$\frac{e + p}{\rho} = \frac{\gamma}{\gamma - 1} p/\rho + u^2/2 = \text{const.} \quad (5.2)$$

along the wall, which permits us to determine u once p and ρ are known.

Our initial conditions consist of the shock jump of the exact solution oriented at an angle of 45° to the computing grid.

Figure 5a is a three-dimensional plot of the density over a 10° wedge at Mach 2 computed using the first order method of Osher and Solomon [11]. Figure 5b is a density profile along the line indicated by an arrow in Figure 5a. The shock angle is approximately 30° . The 30° shock was very difficult for any method to resolve as can be seen by the fact that the shock

is spread over many grid points. This is not an acceptable solution.

To be fair we note that the results shown for the Osher-Solomon method are typical of results for first order upwind schemes. All first order upwind schemes have difficulty with weak, oblique shocks and the Osher-Solomon method has no more difficulty than any other.

Figures 6a and 6b show the results of computations of the flow over a 10^0 wedge at Mach 2 using the second order upwind method of van Leer described in [14] and [15]. The numerical flux for this method is based on the flux vector splitting formulas, described in Section 2, applied to a second order approximation to the dependent variables. A slope limiting function is used to prevent the oscillations which usually occur when shocks are computed using second order methods. These results show that the scheme is monotonic and that it spreads the shock over approximately five grid points in this case.

Figures 7a and 7b illustrate an ideal situation. These results were computed using the rotated finite difference scheme of Section 3 with the exact shock angle specified and the parameter Q set to zero. In this case the shock is confined to between two and three grid points. In [16] van Leer shows that flux vector splitting requires two grid points to resolve steady one-dimensional shocks. This leads us to believe that the results shown are the best that can be expected for a two dimensional method based on these numerical flux formulas. These results also indicate that the assumptions used to derive this method are reasonable.

Unfortunately, when we select the shock angle by the algorithm of Section 4, the method is unstable when $Q=0$. We suspect that this is due to the spacial variations of the computed shock angle since these were not taken into account when the method was derived. We are presently trying to account for this.

At this time we can draw no specific conclusions as to the proper choice for the parameter Q . Extensive numerical experimentation indicates that the choice

$$Q_{i+1/2, j} = \frac{v'_{i, j} + v'_{i+1, j}}{2} \frac{\Delta t}{\Delta x} \quad (5.3)$$

is stable. Figures 8a and 8b demonstrate the performance of this choice combined with the automatic angle method of Section 4. The shock is confined to approximately three grid points.

The second problem that we study is the regular reflection of a shock from a plane wall. The physical situation is shown in Figure 9.

The computations shown below were made on a 61 x 21 uniform grid. Exact values of all variables were specified on the left and top boundaries. All variables were extrapolated at the right boundary and the wall boundary conditions described above were imposed on the lower boundary.

The initial conditions imposed consisted of two shocks which had the same jumps as the exact solution but were located in the wrong place.

Figure 10a is a carpet plot of the density for this flow as computed using the first order method of Osher and Solomon. Figure 10b is a section of this plot taken at $y = .25$. These pictures show that this method smears the shocks so badly that, at $y = .25$, they cannot be distinguished.

Figures 11a and 11b are the corresponding density plots for this flow as computed using the second order upwind method of van Leer. These results are much better than the previous ones. Here we can distinguish two distinct shocks. The first one is spread over between four and five mesh points and the second one is spread over between six and seven mesh points.

Finally, in Figures 12a and 12b, we show density plots for this flow computed using the first order rotated method. This method spreads the first

shock over between two and three mesh points and the second shock over between five and six mesh points. There is a slight undershoot in front of the first shock.

At first sight, these results might appear to be less than dramatic but we should note that we have been comparing a first order method with one of the more sophisticated of second order methods. Under these circumstances, we are encouraged by the fact that the first order method consistently resolved steady oblique shocks within fewer mesh intervals than the second order method. This confirms that our oblique shock model works. With additional effort we can make it work better.

6. Summary and Discussion

In this paper we describe a method which determines the orientation of possible shock solutions to the Euler equations. In addition we show how this information can be used to construct a first order upwind method which computes solutions with greatly improved steady shock resolution. Indeed, we have shown that our first order method resolves steady shocks within fewer mesh intervals than a sophisticated second order upwind method.

This work has shown that the shock resolving ability of numerical methods for hyperbolic equations can be improved if the methods take the orientation of possible shocks into account. Although the results thus far have been encouraging, we wish to improve the present method. Before this can be done some questions need to be answered. In particular, we wish to understand how the variation in angle affects the performance of the method and how we should select the parameter Q in the tangential flux. At present this parameter is selected in an ad hoc manner. It is also important that we construct a

careful stability analysis for this method and that we study appropriate choices for boundary conditions. It might also be helpful to study other choices of upwind formulas for the normal flux.

On a more practical level, we realize that first order methods are usually not accurate enough in regions of smoothly varying flow to be useful in applications. Therefore we are presently developing a second order accurate version of our method. This work will be described in a future paper.

Acknowledgement

I would like to thank Stanley Osher and Bram van Leer for many stimulating discussions on upwind schemes and for their encouragement during this work. I would also like to thank John Strikwerda for providing the simple derivation of equation (4.2) which appears in this paper.

References

- (1) Chakravarthy, S. and Osher, S., "Numerical Experiments with the Osher Upwind Scheme for The Euler Equations.", AIAA Paper 82-0975, AIAA/ASME 3rd Joint Thermophysics, Plasma and Heat Transfer Conference, June, 1982.
- (2) Godunov, S. K., "A Finite Difference Method for the Numerical Computation of Discontinuous Solutions of the Equations of Fluid Dynamics.", Mat. Sb. Vol. 47, 1959, (in Russian) ,also Cornell Aeronautical Lab (CALSPAN) Translation.
- (3) Harten, A. and Hyman, J. M., "A Self-Adjusting Grid for the Computation of Weak Solutions Of Hyperbolic Conservation Laws.", Report LA9105, Center for Nonlinear Studies, Theoretical Division, Los Alamos National Lab, Los Alamos, N.M., (1981)
- (4) Harten, A. ,Lax, P. D., and van Leer, B., "On Upstream Differencing and Godunov-Type Schemes for Hyperbolic Conservation Laws.", SIAM Rev., Vol. 25, pp. 35-62, 1983.
- (5) Harten, A., "High Resolution Schemes for Hyperbolic Conservation Laws.", J. Comp. Phys., Vol. 49, pp. 357-393, 1983.
- (6) Jameson, A., "Iterative Solution of Transonic Flows over Airfoils and Wings, Including Flows at Mach 1.", Comm. Pure Appl. Math., Vol. XXVII, pp. 283-309, 1974.

- (7) Lax, P. and Wendroff, B. "Systems of Conservation Laws", Comm. Pure Appl. Math., Vol. XIII, pp. 217-237, 1960.
- (8) Lax, P. D., Hyperbolic Systems of Conservation Laws and the Mathematical Theory of Shock Waves. SIAM, Philadelphia, 1972.
- (9) Liepmann, H. W. and Roshko, A., Elements of Gasdynamics, J. Wiley and Sons, New York, 1957.
- (10) Murman, E. M., "Analysis of Embedded Shock Waves Calculated by Relaxation Methods.", AIAA J., Vol. 12, pp. 626-633, 1974.
- (11) Osher, S. and Solomon, F., "Upwind Difference Schemes for Hyperbolic Systems of Conservation Laws.", Math. Comp. Vol. 38, pp. 339-374, 1982.
- (12) Roe, P. L., "Approximate Riemann Solvers, Parameter Vectors and Difference Schemes," J. Comp. Phys., Vol. 43, pp. 357-372, 1981.
- (13) Segel, L. A., Mathematics Applied to Continuum Mechanics, Macmillan Publishing Co., New York, 1977.
- (14) van Albada, G. D., van Leer, B. and Roberts, W. W., "A Comparative Study of Computational Methods in Cosmic Gas Dynamics.", ICASE Report 81-24, 1981.

- (15) van Leer, B., "On the Relation Between the Upwind-Differencing Schemes of Godunov, Enquist-Osher and Roe.", ICASE Report 81-11, 1981.
- (16) van Leer, B., "Flux Vector Splitting for the Euler Equations.", ICASE Report 82-30, 1982.
- (17) Woodward, P. and Colella, P., in Proceedings, 7th Int. Conf. Numer. Methods in Fluid Dynamics, Stanford/NASA Ames, 1980.
- (18) Yee, H. C., Warming, R. F. and Harten, A., "On the Application and Extension of Harten's High Resolution Scheme.", NASA TM 84256, 1982.

Table I

| Angle Range | $G^+(U'_{i,j}, U'_{i,j\pm 1})$ | $G^-(U'_{i+1,j}, U'_{i+1,j\pm 1})$ | $G^+(U'_{i,j}, U'_{i\pm 1,j})$ | $G^-(U'_{i,j+1}, U'_{i\pm 1,j+1})$ |
|---|--------------------------------|------------------------------------|--------------------------------|------------------------------------|
| $-\infty < \text{Tan}\theta < -\frac{\Delta y}{\Delta x}$ | $G^-(U'_{i,j})$ | $G^-(U'_{i+1,j})$ | $G^-(U'_{i-1,j})$ | $G^-(U'_{i+1,j+1})$ |
| $-\frac{\Delta y}{\Delta x} < \text{Tan}\theta < 0$ | $G^-(U'_{i,j-1})$ | $G^-(U'_{i+1,j+1})$ | $G^-(U'_{i,j})$ | $G^-(U'_{i,j+1})$ |
| $0 < \text{Tan}\theta < \frac{\Delta y}{\Delta x}$ | $G^-(U'_{i,j+1})$ | $G^-(U'_{i+1,j-1})$ | $G^-(U'_{i,j})$ | $G^-(U'_{i,j+1})$ |
| $\frac{\Delta y}{\Delta x} < \text{Tan}\theta < \infty$ | $G^-(U'_{i,j})$ | $G^-(U'_{i+1,j})$ | $G^-(U'_{i+1,j})$ | $G^-(U'_{i-1,j+1})$ |

Figure Captions

- Figure 1. Geometry of local and global coordinate systems.
- Figure 2. Construction of tangential flux.
- Figure 3. Oblique shock problem in physical domain.
- Figure 4. Oblique shock problem in computational domain.
- Figure 5a. Three dimensional plot of density for oblique shock problem, computed using the method of Osher and Solomon.
- Figure 5b. Density profile six grid points from the wall for the oblique shock problem, computed using the method of Osher and Solomon.
- Figure 6a. Three dimensional plot of density for oblique shock problem, computed using the second order method of van Leer.
- Figure 6b. Density profile six grid points from the wall for the oblique shock problem, computed using the second order method of van Leer.
- Figure 7a. Three dimensional plot of density for oblique shock problem, computed using rotationally biased differences with exact shock angle.

Figure 7b. Density profile six grid points from the wall, computed using rotationally biased differences with exact shock angle.

Figure 8a. Three dimensional plot of density for oblique shock problem computed using rotationally biased differences with automatic angle algorithm.

Figure 8b. Density profile six grid points from the wall computed using rotationally biased differences with automatic angle algorithm

Figure 9. Shock reflection problem.

Figure 10a. Three dimensional plot of density for shock reflection problem computed using the method of Osher and Solomon.

Figure 10b. Density profile at $y = .25$ for shock reflection problem computed using the method of Osher and Solomon.

Figure 11a. Three dimensional plot of density for shock reflection problem computed using the second order method of van Leer.

Figure 11b. Density profile at $y = .25$ for shock reflection problem computed using the second order method of van Leer.

Figure 12a. Three dimensional plot of density for shock reflection problem computed using rotationally biased differences with automatic angle algorithm.

Figure 12b. Density profile at $y = .25$ for shock reflection problem computed using rotationally biased differences with automatic angle algorithm.

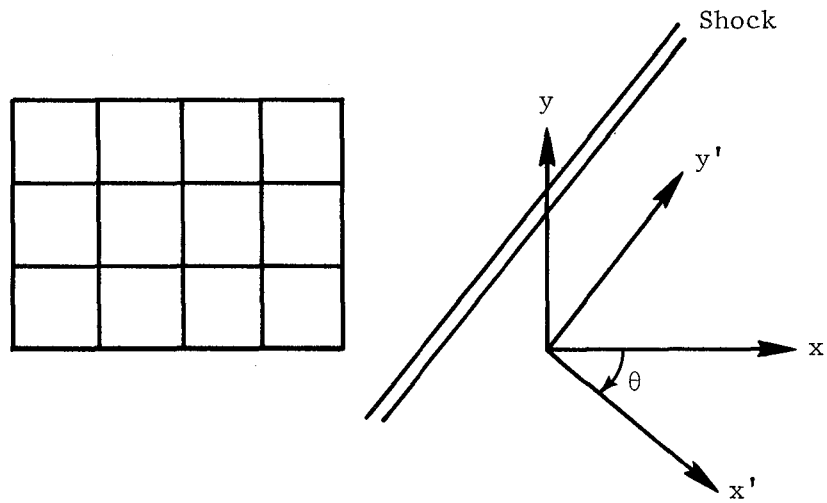


Figure 1.

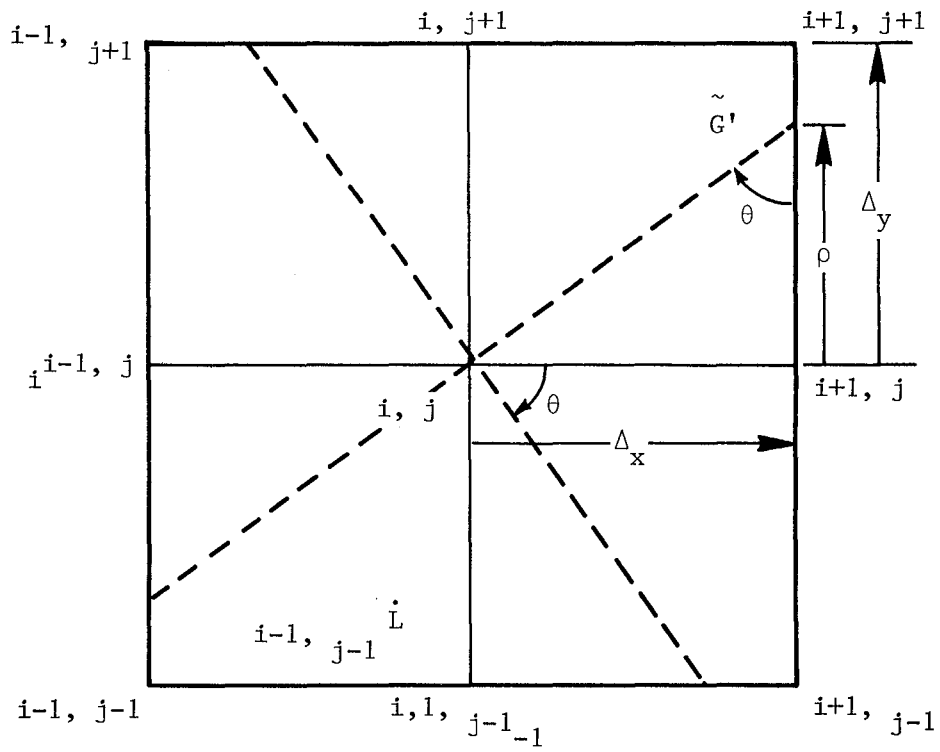


Figure 2.

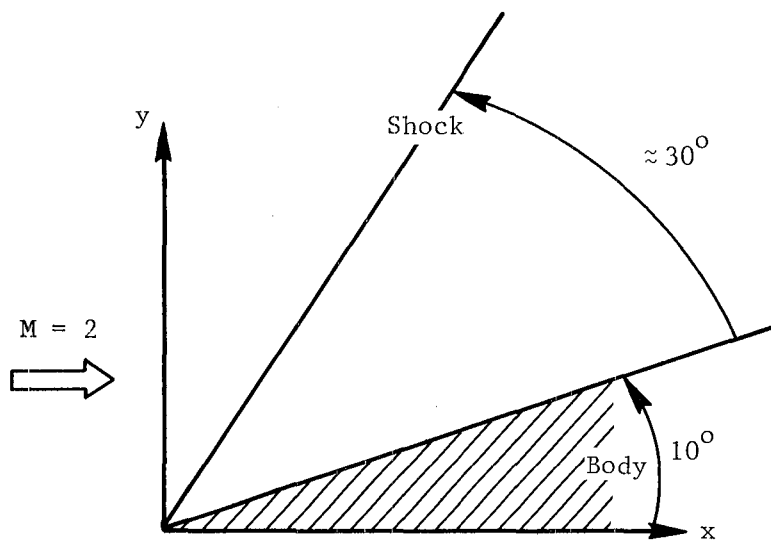


Figure 3.

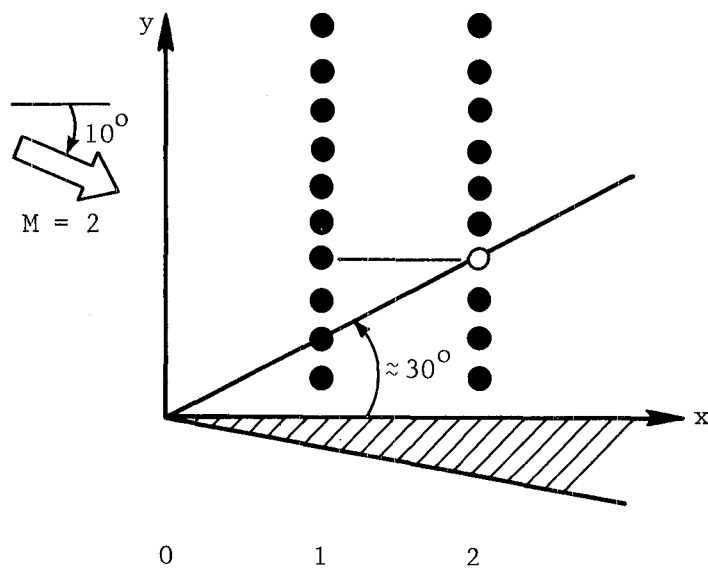


Figure 4.

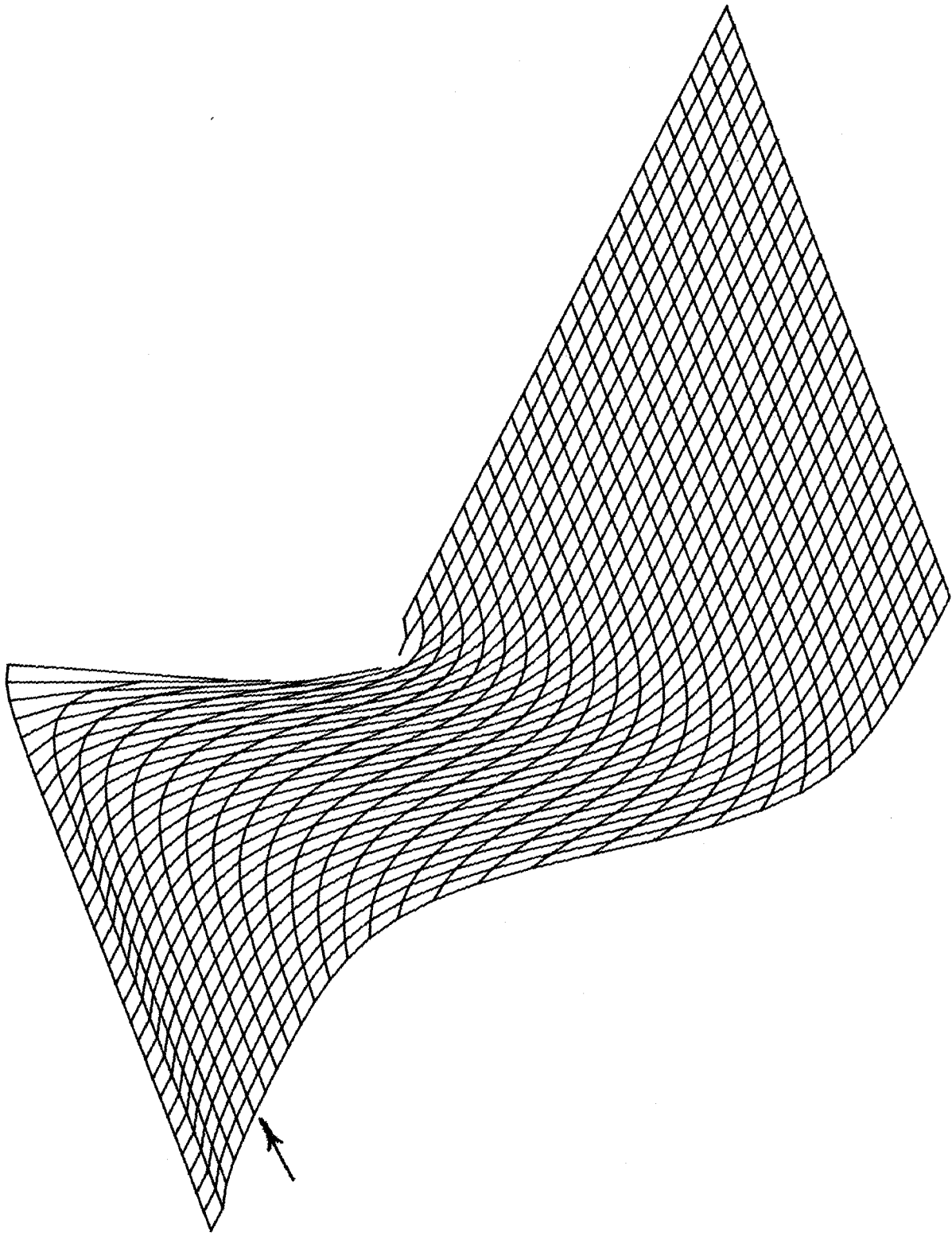


Figure 5a.

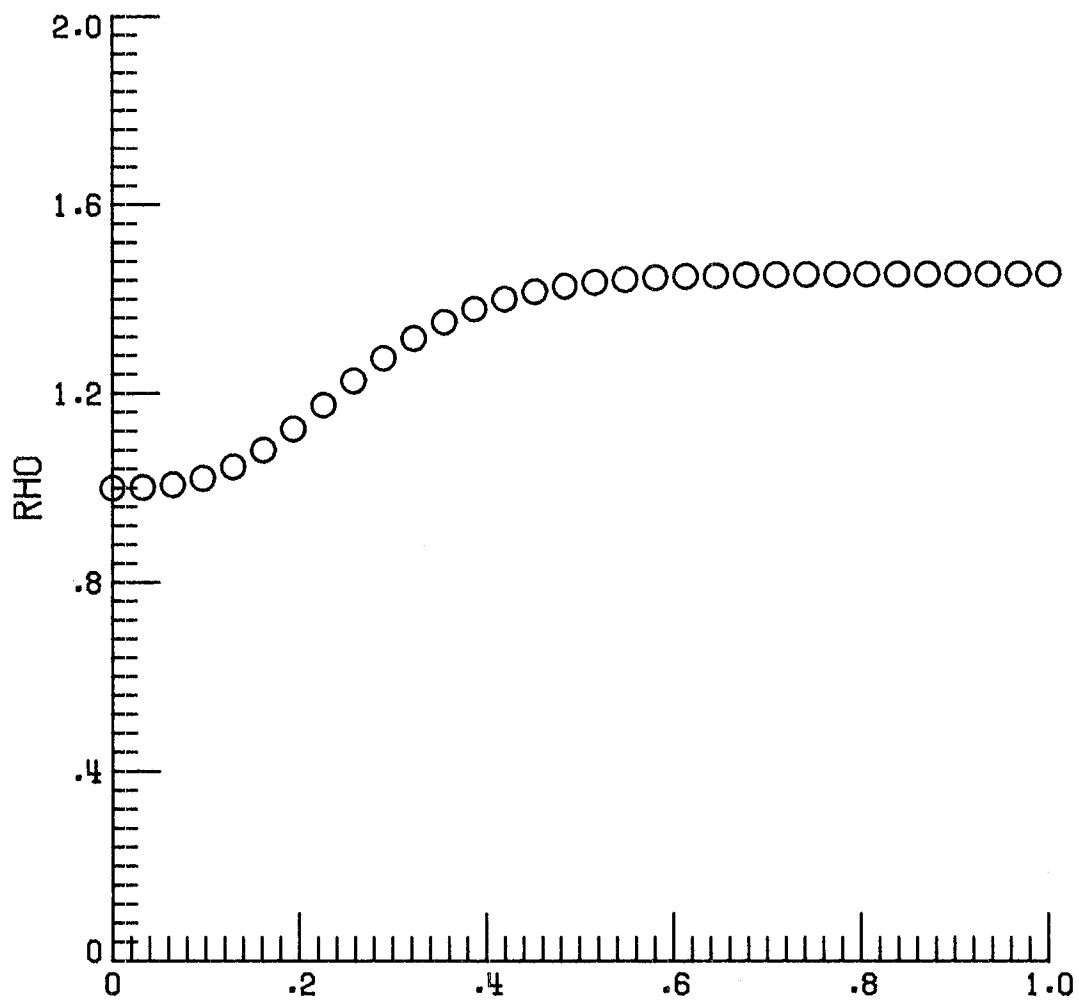


Figure 5b.

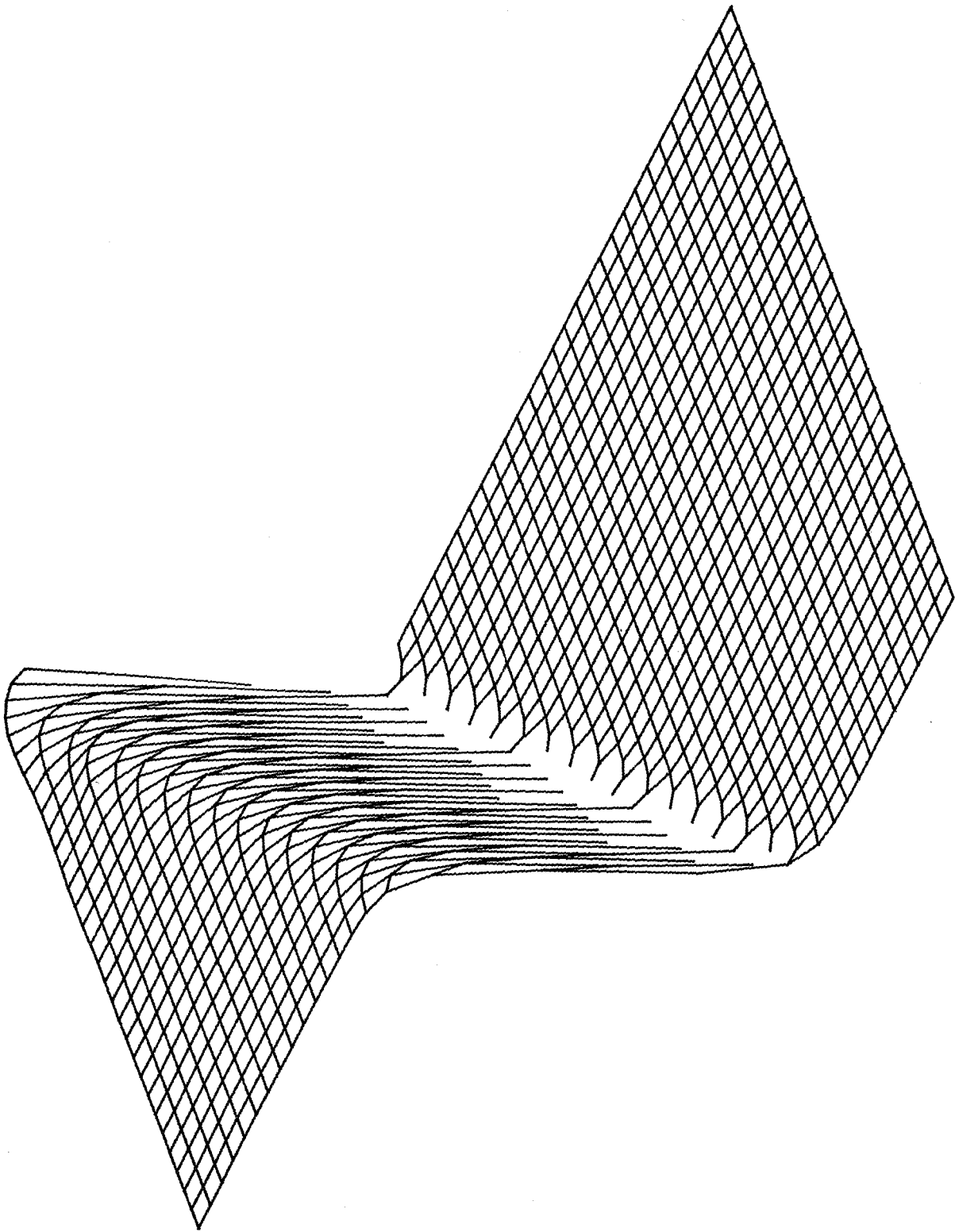


Figure 6a.

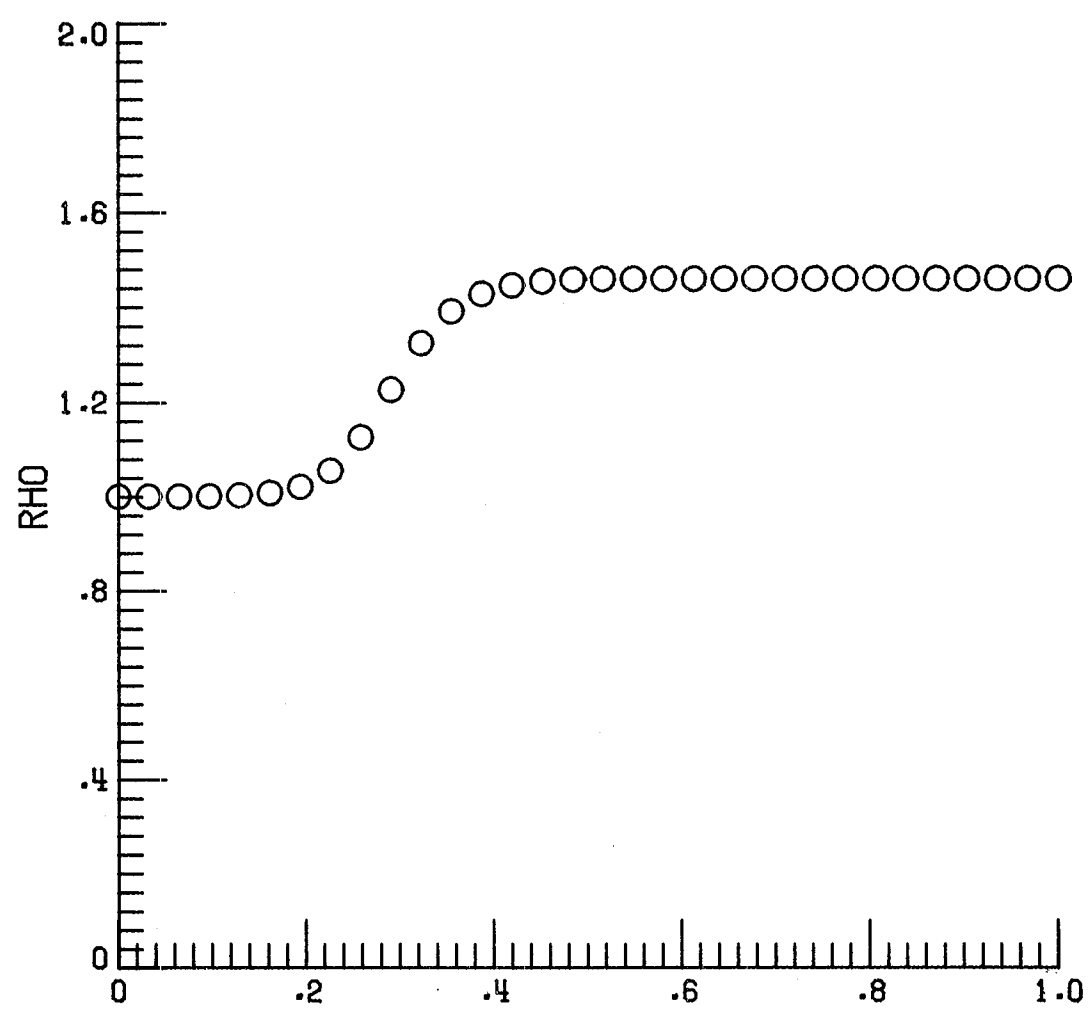


Figure 6b.

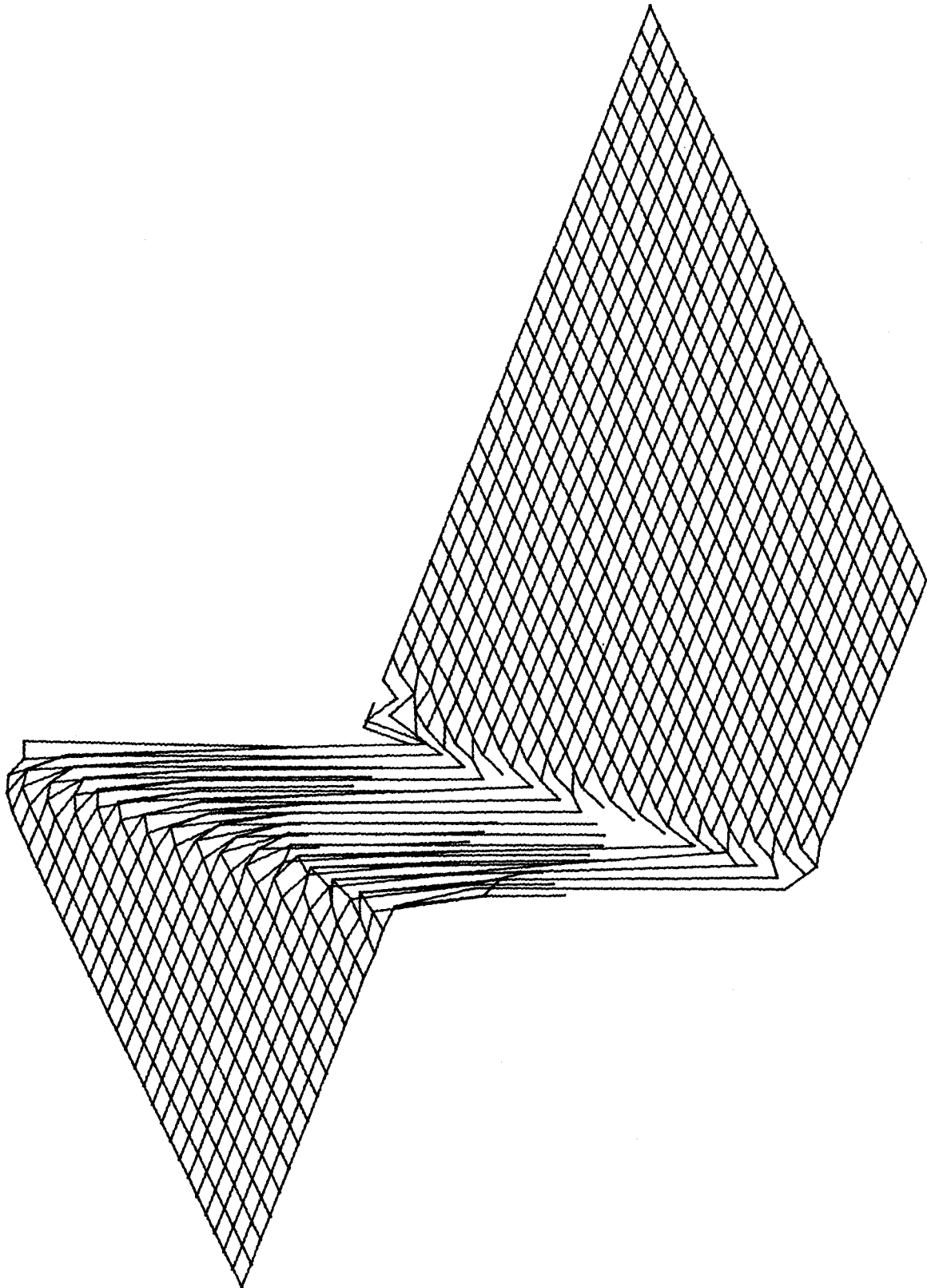


Figure 7a.

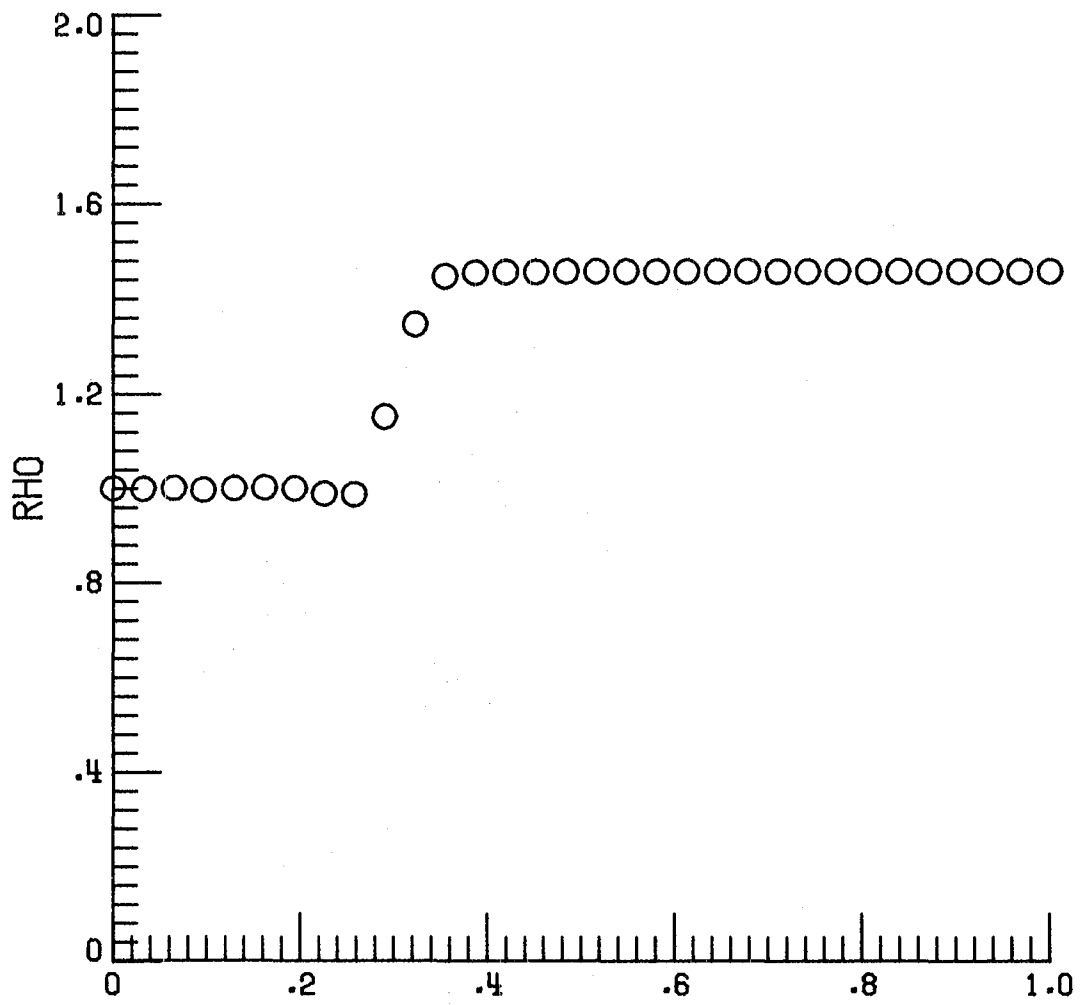


Figure 7b.

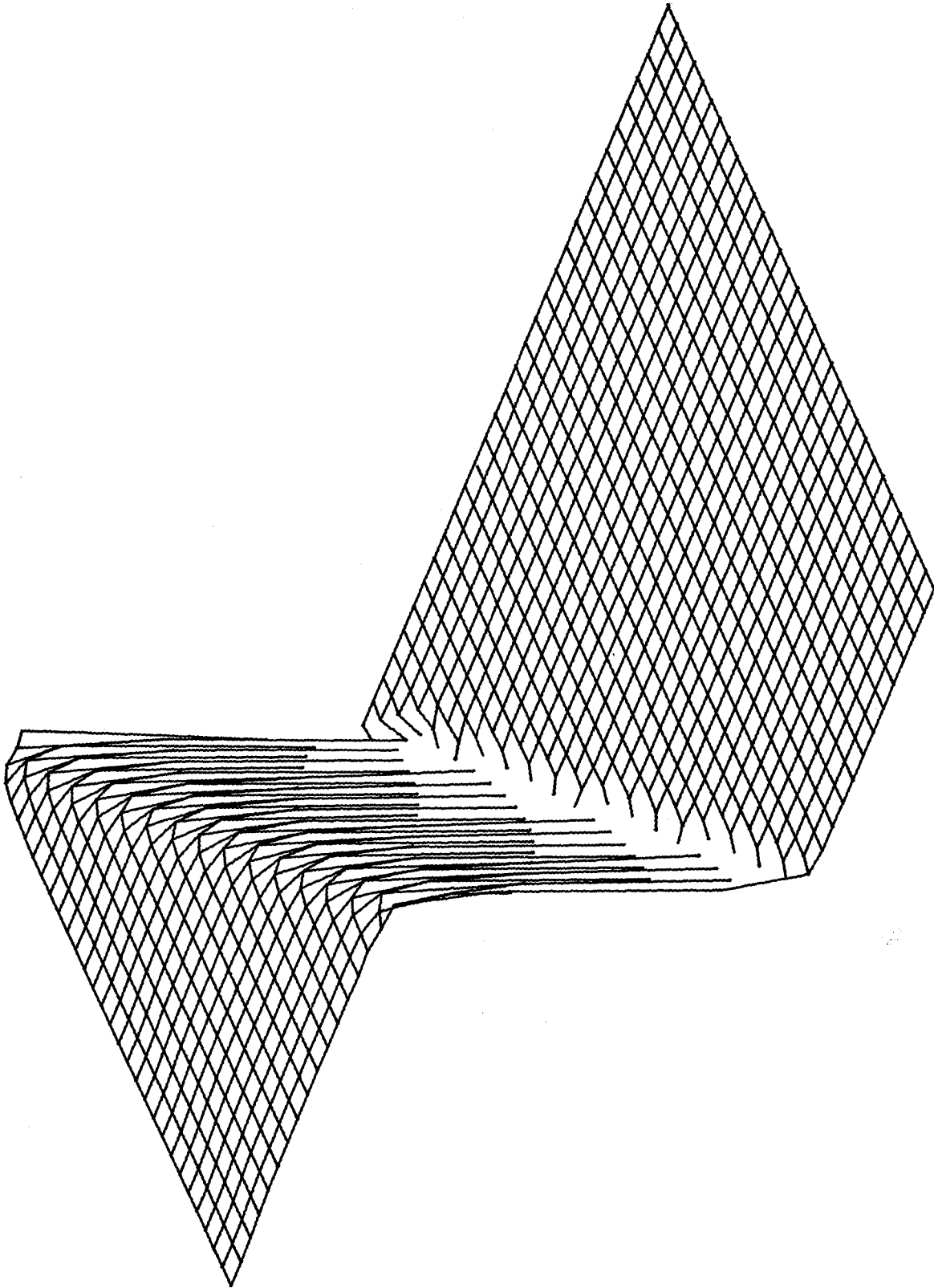


Figure 8a.

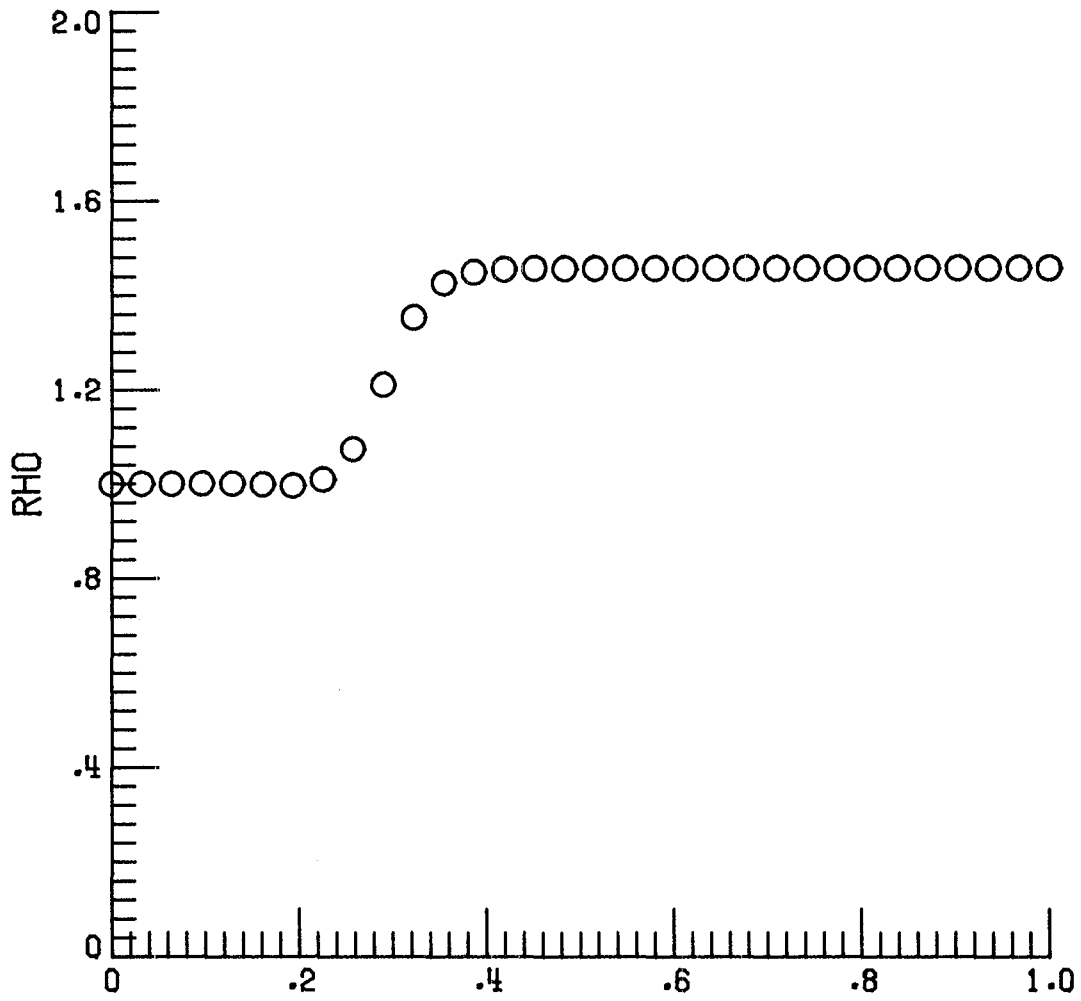


Figure 8b.

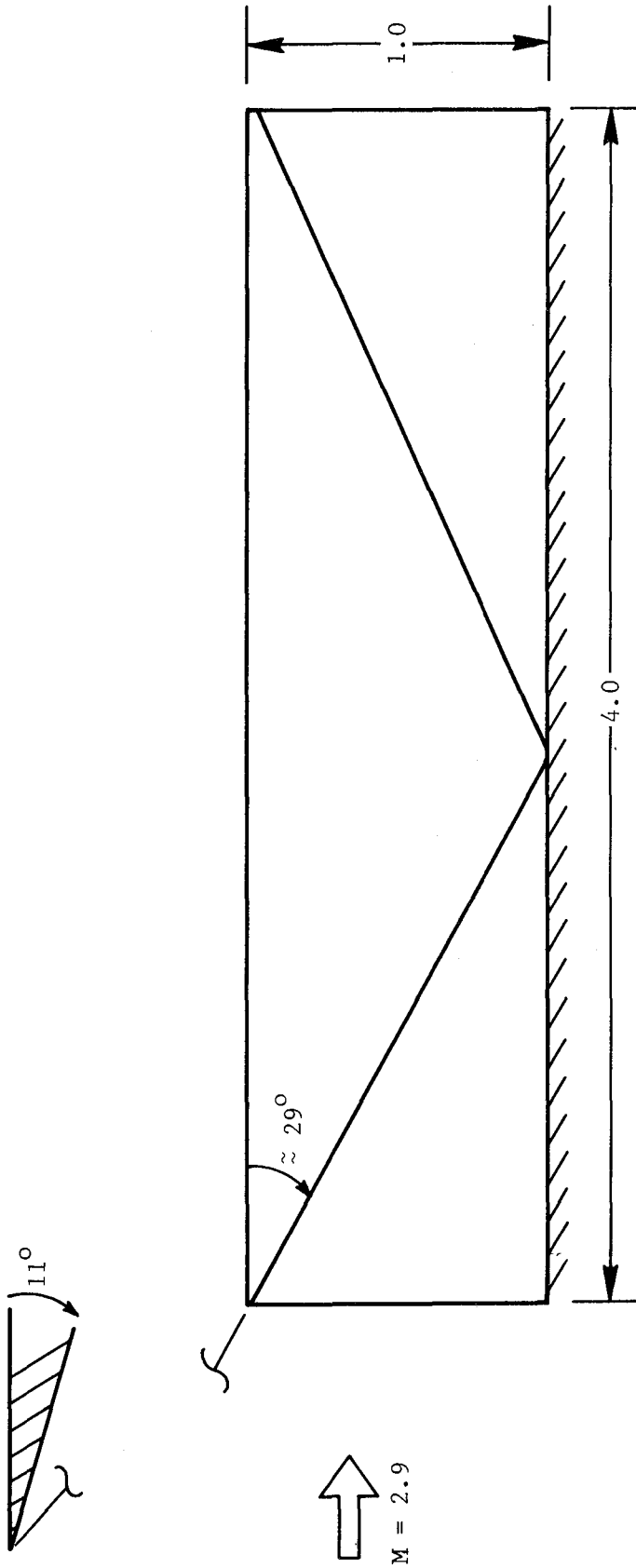


Figure 9.

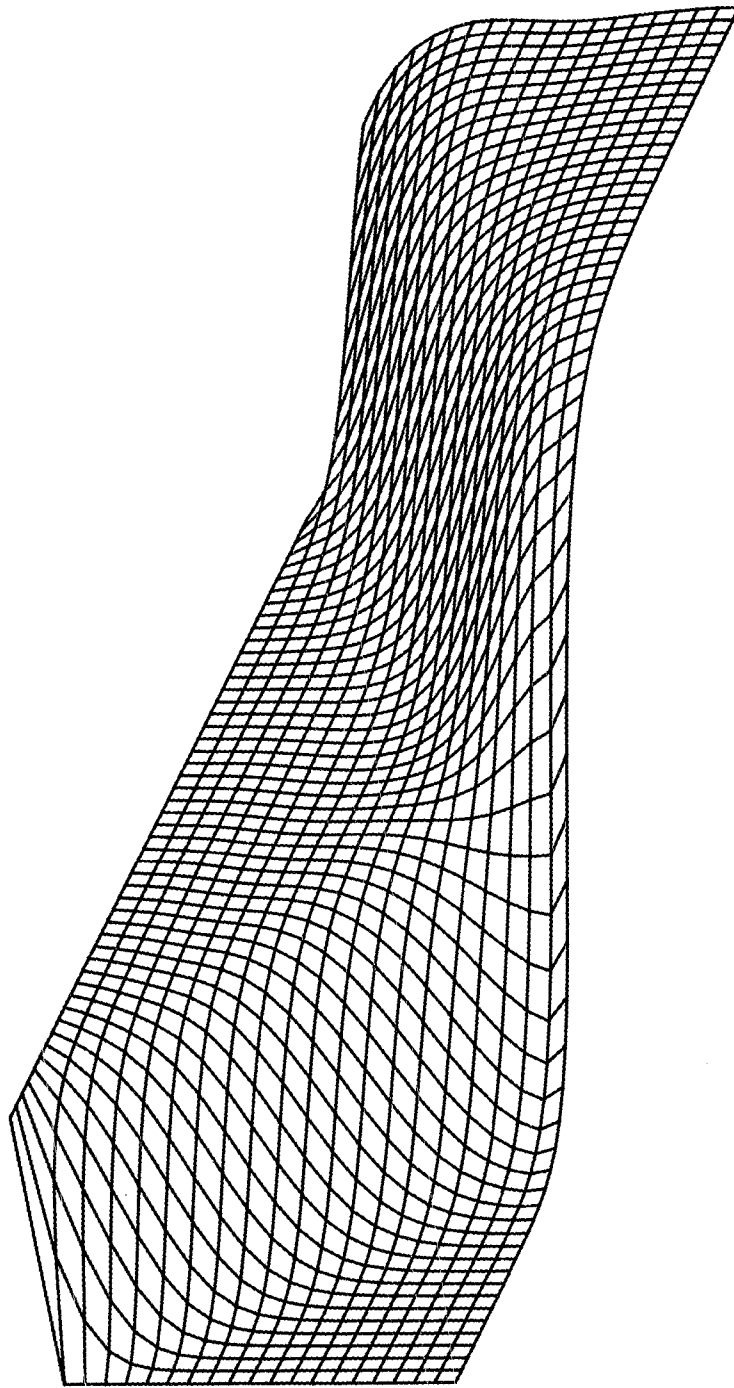


Figure 10a.

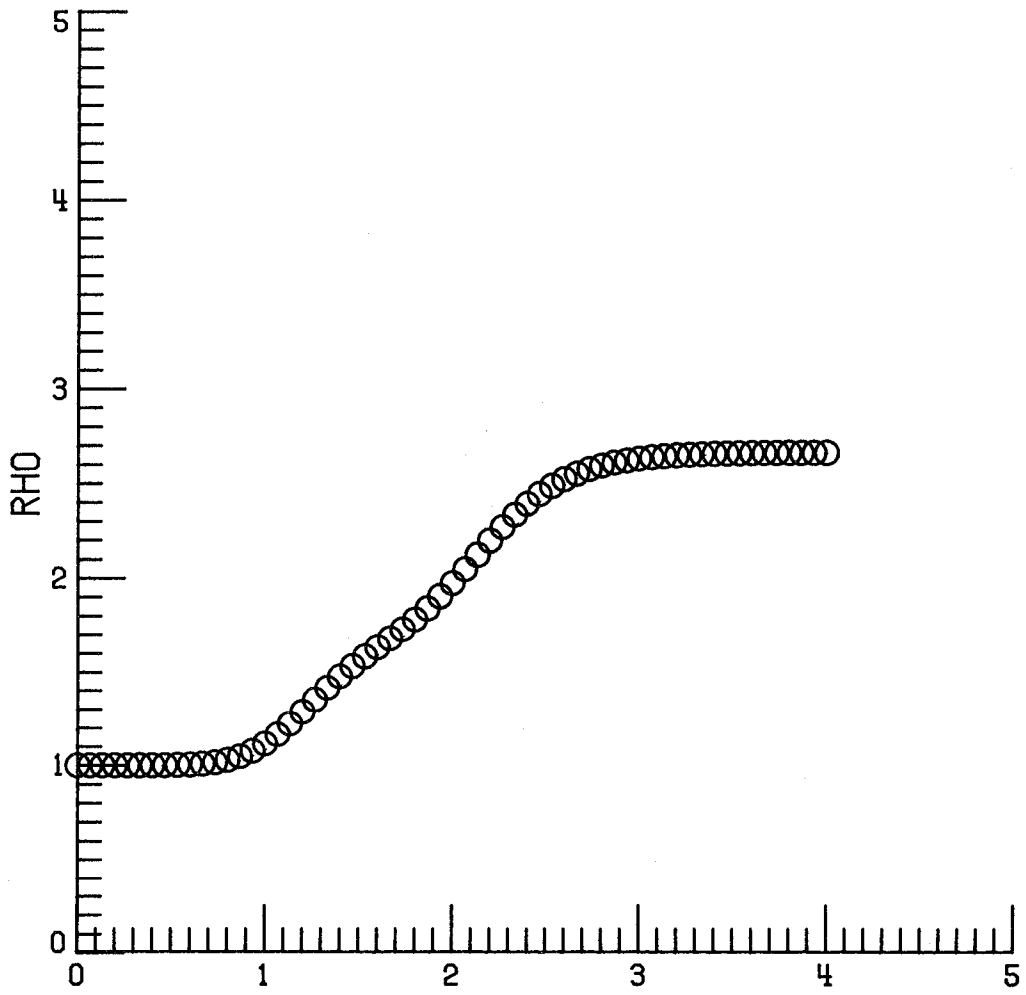


Figure 10b.

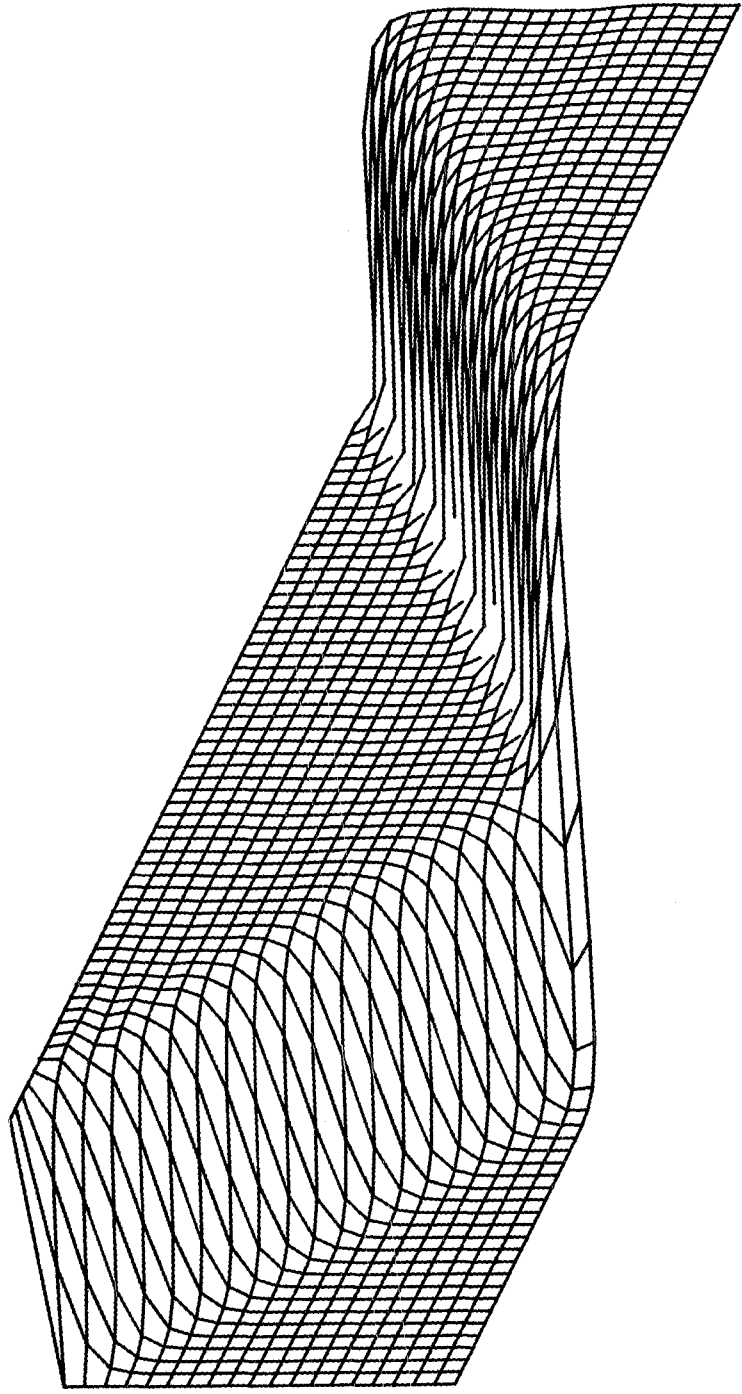


Figure 11a.

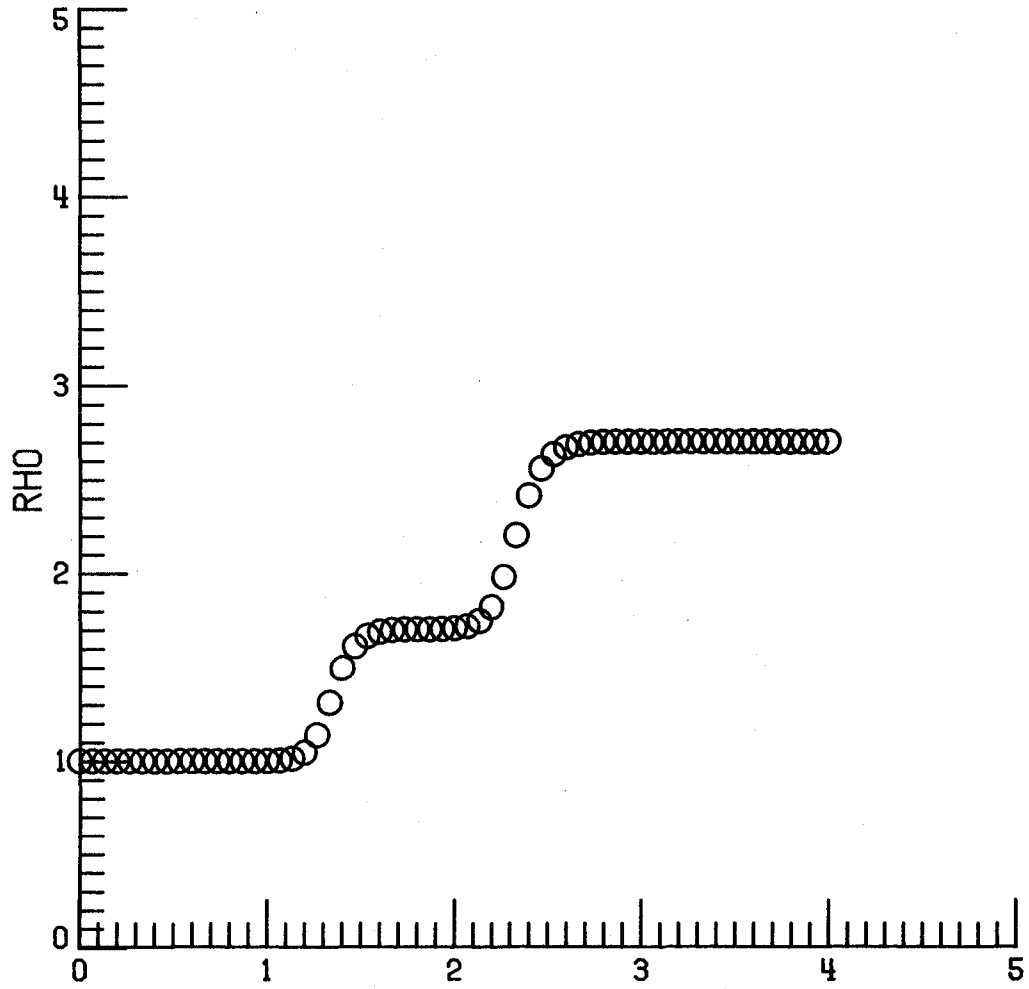


Figure 11b.

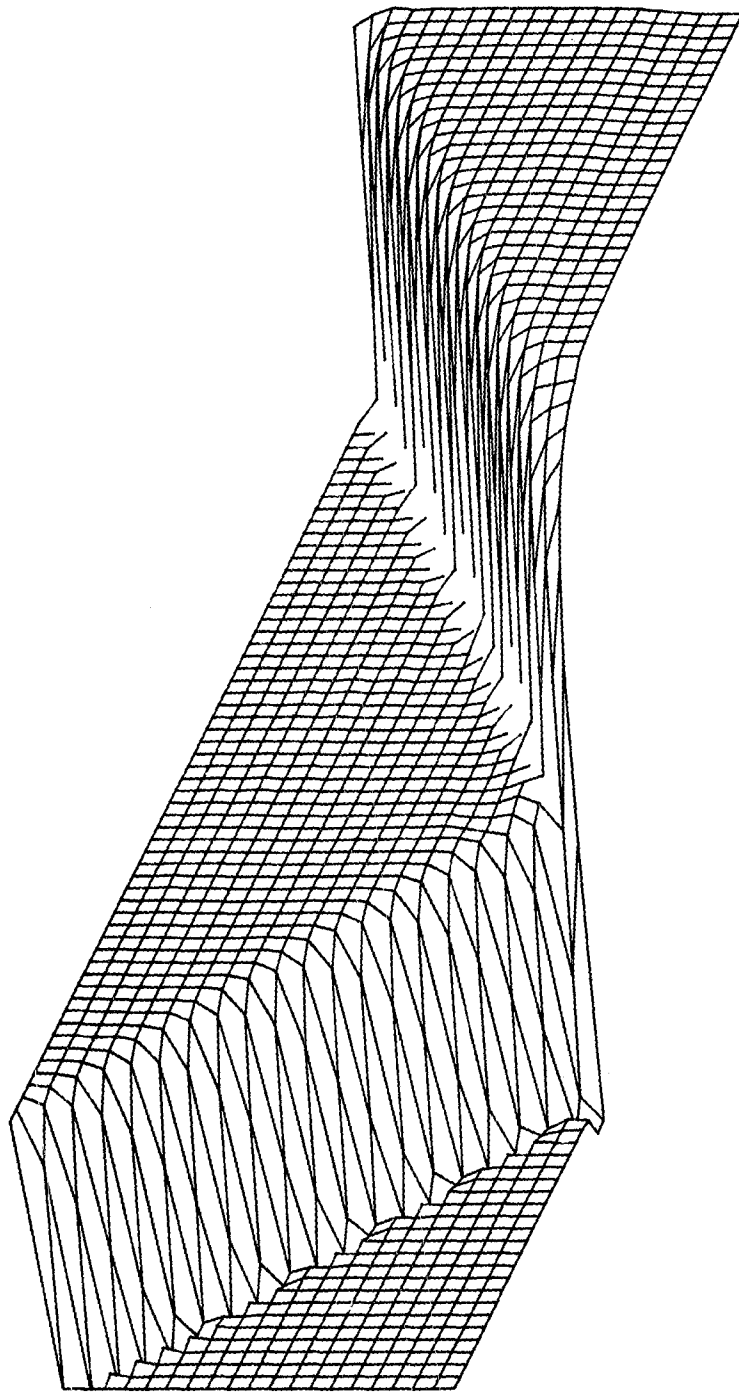


Figure 12a.

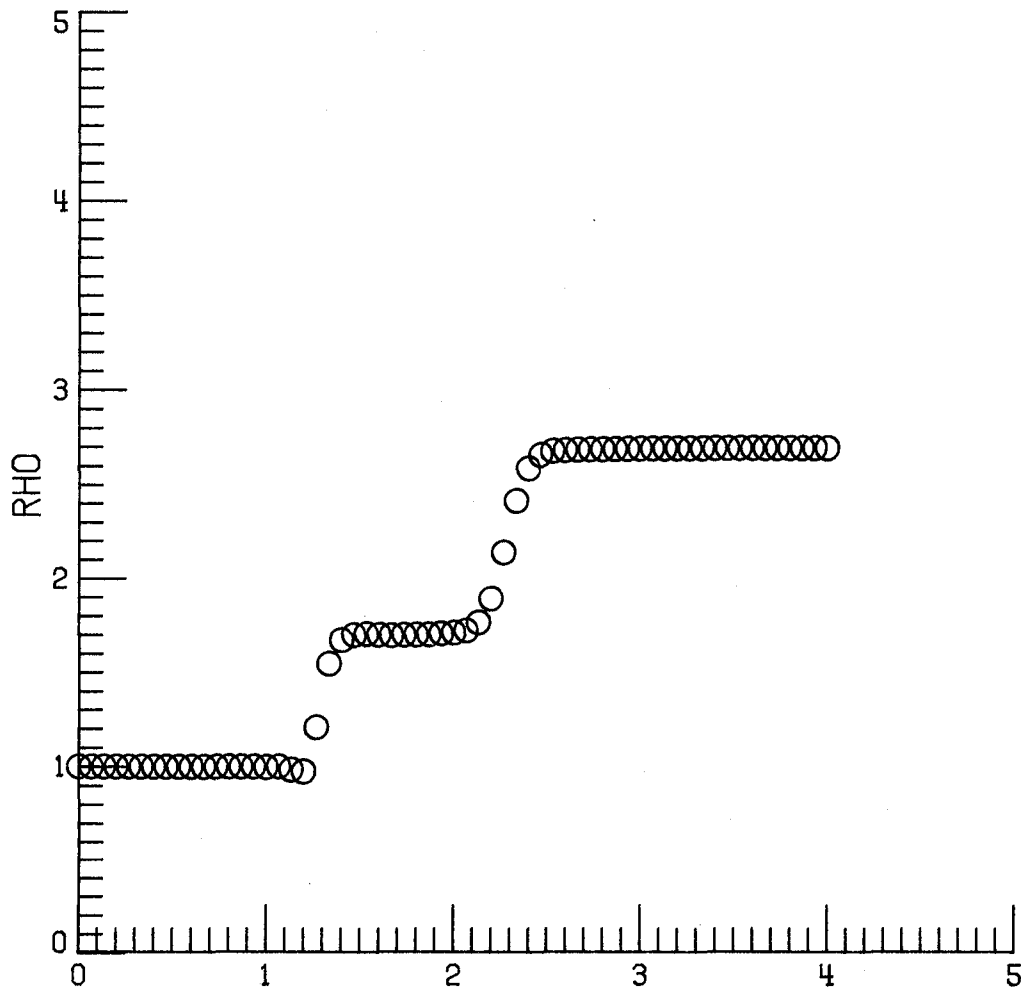


Figure 12b.

| | | | | | |
|--|--|-----------------------------|---|--|--|
| 1. Report No. NASA CR-172179 | | 2. Government Accession No. | | 3. Recipient's Catalog No. | |
| 4. Title and Subtitle A Rotationally Biased Upwind Difference Scheme for the Euler Equations | | | | 5. Report Date July 1983 | |
| | | | | 6. Performing Organization Code | |
| 7. Author(s) Stephen F. Davis | | | | 8. Performing Organization Report No. 83-37 | |
| 9. Performing Organization Name and Address Institute for Computer Applications in Science and Engineering Mail Stop 132C, NASA Langley Research Center Hampton, VA 23665 | | | | 10. Work Unit No. | |
| | | | | 11. Contract or Grant No. NAS1-17070 | |
| | | | | 13. Type of Report and Period Covered Contractor report | |
| 12. Sponsoring Agency Name and Address National Aeronautics and Space Administration Washington, D.C. 20546 | | | | 14. Sponsoring Agency Code | |
| 15. Supplementary Notes Langley Technical Monitor: Robert H. Tolson Final Report | | | | | |
| 16. Abstract The upwind difference schemes of Godunov, Osher, Roe and van Leer are able to resolve one-dimensional steady shocks for the Euler equations within one or two mesh intervals. Unfortunately, this resolution is lost in two dimensions when the shock crosses the computing grid at an oblique angle. To correct this problem, we develop a numerical scheme which automatically locates the angle at which a shock might be expected to cross the computing grid and then constructs separate finite difference formulas for the flux components normal and tangential to this direction. We present numerical results which illustrate the ability of this new method to resolve steady oblique shocks. | | | | | |
| 17. Key Words (Suggested by Author(s)) finite difference methods Euler equations shock waves | | | 18. Distribution Statement 64 Numerical Analysis Unclassified-Unlimited | | |
| 19. Security Classif. (of this report) Unclassified | 20. Security Classif. (of this page) Unclassified | 21. No. of Pages 52 | 22. Price A04 | | |

End of Document